Supplementary Information

Structure of Trypanosome Coat Protein VSGsur and Function in Suramin Resistance

Johan Zeelen[1*], Monique van Straaten[1*], Joseph Verdi[1,2], Alexander Hempelmann[1], Hamidreza Hashemi[2], Kathryn Perez[3], Philip D. Jeffrey[4], Silvan Hälg[5], Natalie Wiedemar[5,6], Pascal Mäser[5,6], F. Nina Papavasiliou[2], C. Erec Stebbins[1†]

[1]Division of Structural Biology of Infection and Immunity, German Cancer Research Center [2]Division of Immune Diversity, German Cancer Research Center, Heidelberg, Germany. [3]Protein Expression and Purification Core Facility, EMBL Heidelberg, Meyerhofstraße 1, Heidelberg, Germany [4]Department of Molecular Biology, Princeton University, Princeton, New Jersey, USA [6]University of Basel, Basel CH-4001, Switzerland [6]Swiss Tropical and Public Health Institute, Basel CH-4002, Switzerland.

[*]These authors contributed equally to this work.

[†]Correspondence to: e.stebbins@dkfz-heidelberg.de

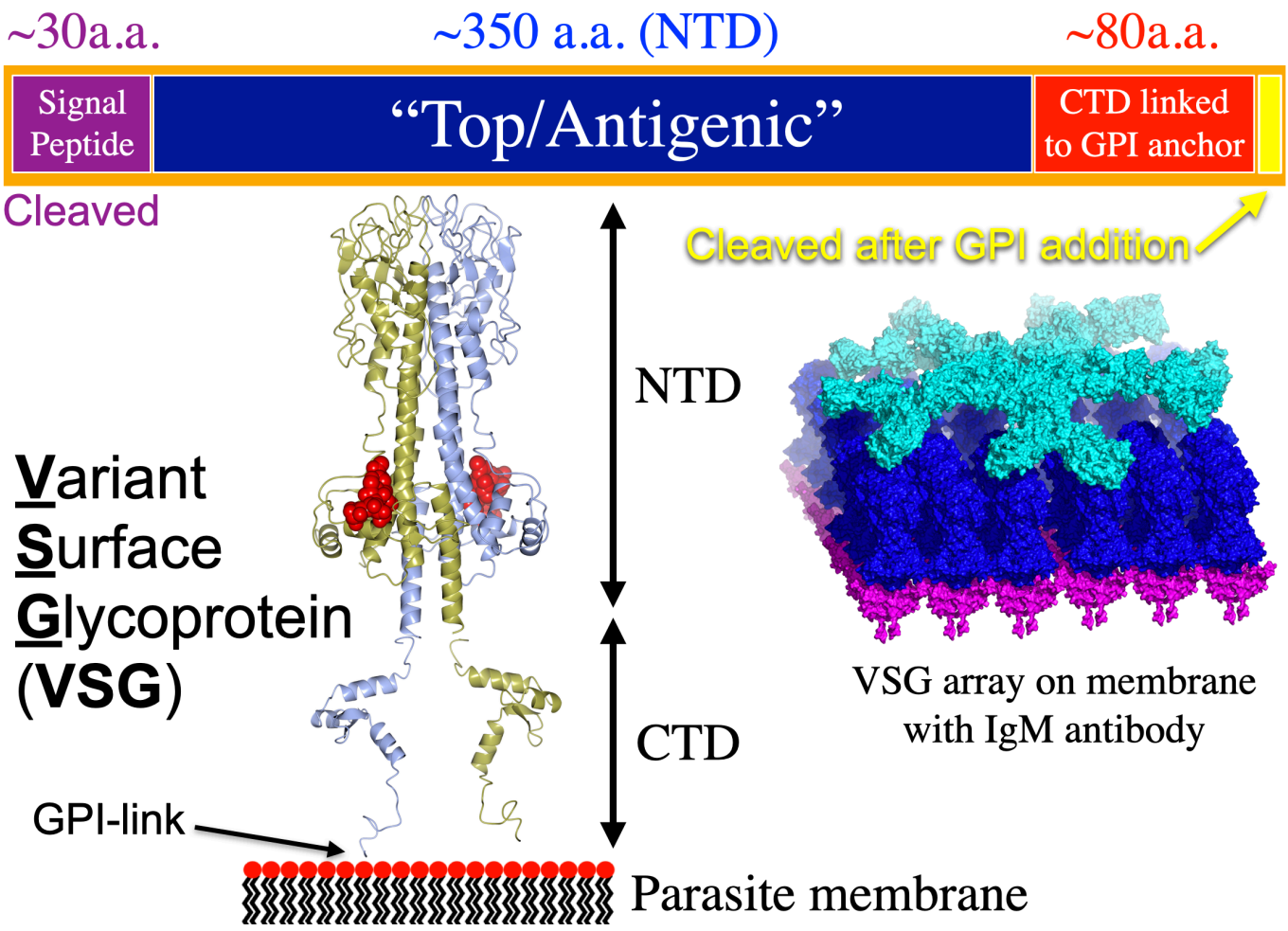

Supplementary Fig. 1: Domain structure of the VSG proteins. The top bar shows a schematic of the domain structure of the VSG coat proteins with rough amino acid size associated with each. The unlabeled yellow region at the far C-terminus represents the peptide cleaved from the end of the immature polypeptide when the GPI-anchor is attached. NTD is the N-terminal domain and CTD is the C-terminal domain. Underneath is the structure of VSG1 schematically represented by a composite model of N and C-terminal domain structures (PDB IDs 5LY9 and 5M4T, respectively[1]), illustrated over a cartoon of the parasite membrane. On the right is a model of an array of VSG proteins (NTD in blue, CTD in magenta) on the surface and interacting with a hypothetical model of immunoglobulin M (IgM shown in cyan).

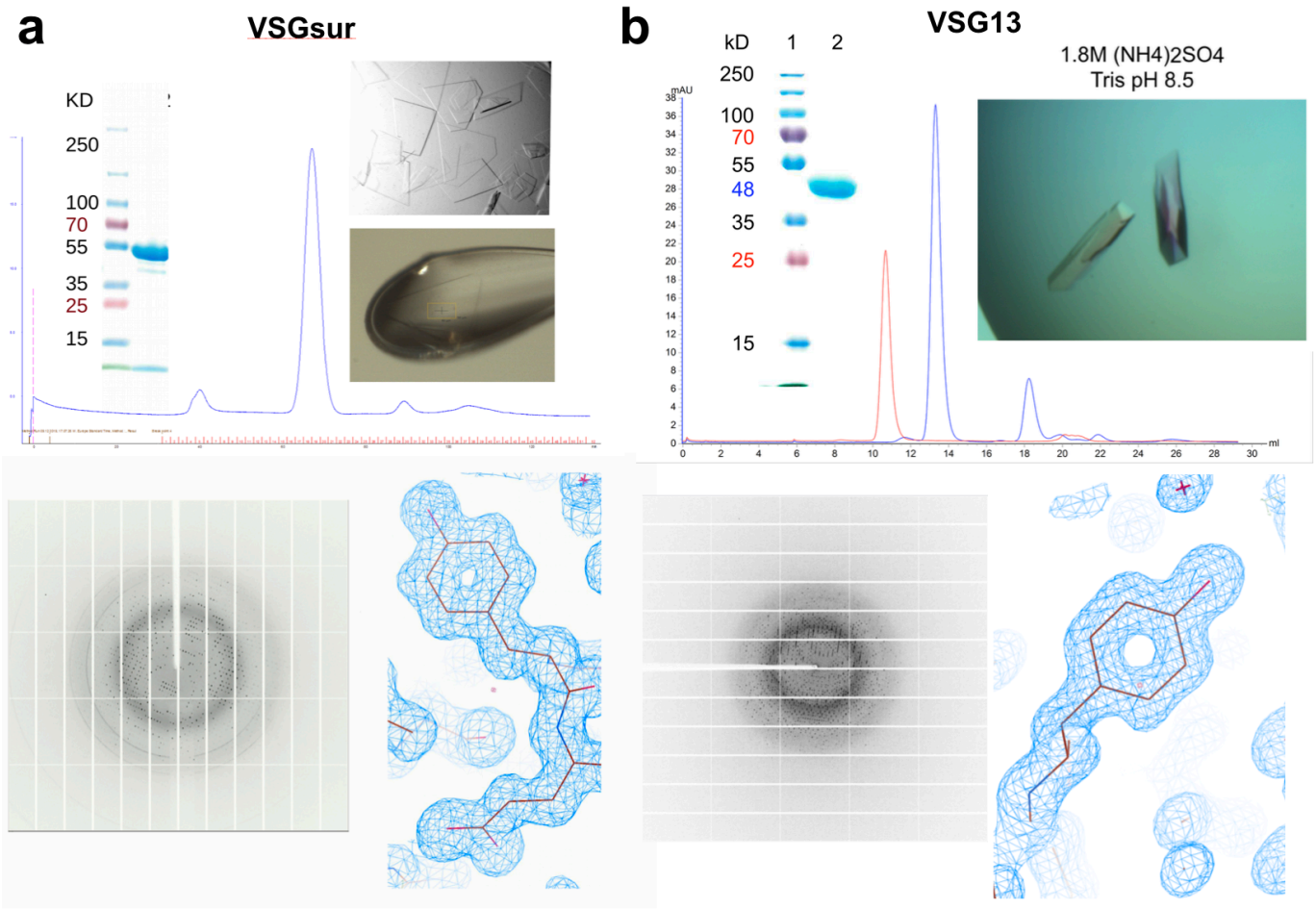

Supplementary Fig. 2: Purification, crystallization, and representative electron density of VSGsur and VSG13. Summary of various steps in the crystallographic structural solution of VSG13 and VSGsur. **(a)** Panels showing the gel filtration chromatogram (Superdex 200, Methods) of purified VSGsur NTD and a coomassie stained SDS-PAGE gel of the final material used for crystallization. Images of cryo-crystals grown in hang-drops and cooled crystals in the X-ray beam, a diffraction image, and final model 2Fo-Fc electron density contoured at 1σ. **(b)** Panels included are: the gel filtration chromatogram (Superdex 200, Methods) of purified VSG13 NTD (native in blue and reductively methylated in red, the latter running larger as perhaps a tetramer but occurring as a dimer in the asymmetric unit of the crystal), a coomassie stained SDS-PAGE gel of the final material used for crystallization, images of crystals prior to harvesting in hanging drops, a diffraction image, and final model 2Fo-Fc electron density contoured at 1σ.

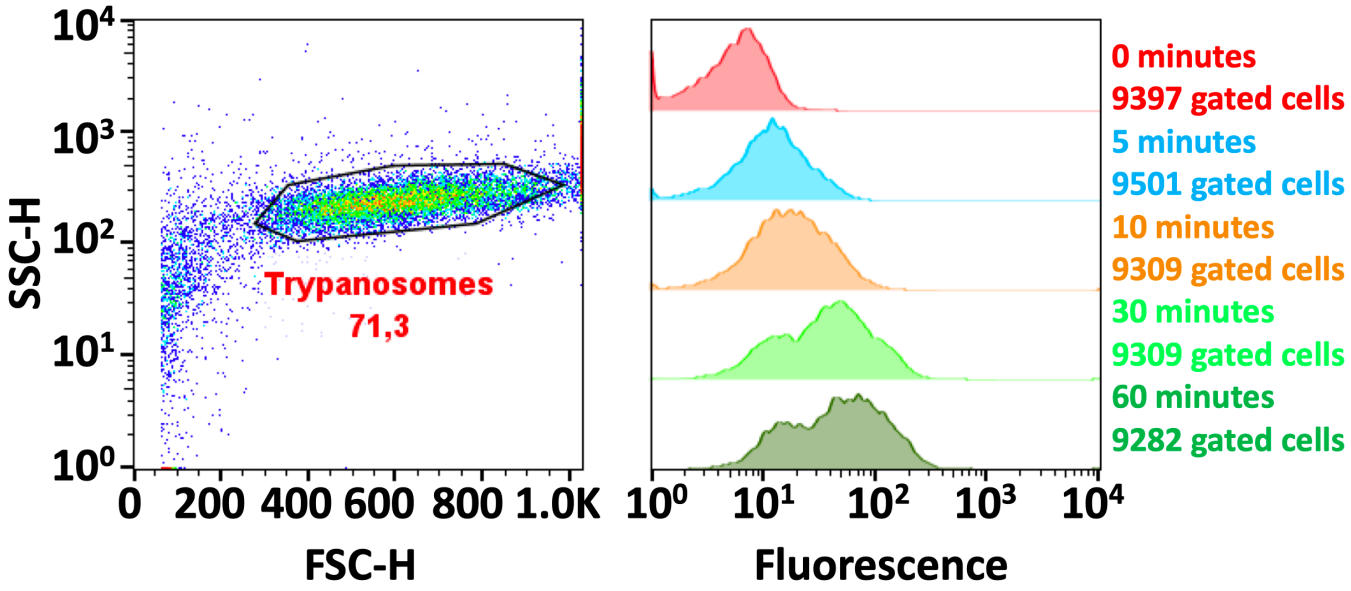

Supplementary Figure 3. Example of the gating and analysis performed prior to the generation of the graphs that compare the uptake rates of the various extracellular molecules between the different trypanosome cell lines. Trypanosomes are selected by forward and side scatter gating, and between 7 and 10 thousand gated cells are counted for each data point.

Supplementary Table 1: Crystallographic Statistics for Wild Type VSGsur

	VSGsur	VSGsur+I3C	VSGsur + 0.77mM suramin
Data Collection			
Beamline	BESSY MX 14.1	BESSY MX 14.2	SLS X06DA
Processing software	XDSAPP	XDSAPP	go.pi
Wavelength (Å)	0.9184	2.066	1.0
Resolution range (Å)	48.05 -1.21 (1.25-1.21)	44.15-1.92 (1.99-1.92)	47.87-1.86 (1.93 -1.86)
Space group	P 21 21 2	P 21 21 2	P 1 21 1
Unit Cell *a*, b, *c* (Å)	47.0 71.0 130.4	46.96 70.89 129.65	52.69 79.22 118.00
Unit Cell α, β, γ (°)	90 90 90	90 90 90	90 90.78 90
Total reflections	747748 (26978)	507768 (5366)	545357 (55408)
Unique reflections	122558 (7073)	27999 (845)	81516 (8077)
Multiplicity	6.1 (3.8)	18.1 (6.4)	6.7 (6.8)
Completeness (%)	91.49 (53.39)	82.57 (25.54)	99.91 (99.77)
Mean *I/sigma(I)*	8.57 (0.38)	13.99 (0.68)	12.25 (2.32)
Wilson B-factor	15.43	30.05	
R-merge	0.09566 (2.578)	0.1762 (1.899)	0.1091 (0.759)
R-meas	0.1044 (2.988)	0.1813 (2.055)	0.1185 (0.8029)
R-pim	0.04114 (1.487)	0.04182 (0.7539)	0.04537 (0.3039)
CC1/2	0.998 (0.174)	0.995 (0.380)	0.997 (0.741)
CC*	0.999 (0.544)	0.999 (0.742)	0.999 (0.923)
Refinement			
Refinement reflections	122545 (7073)	27993 (845)	81516 (8077)
R-free reflections	2100 (121)	1124 (34)	3910 (372)
R-work	0.174 (0.377)	0.235 (0.333)	0.195 (0.297)
R-free	0.184 (0.348)	0.256 (0.382)	0.227 (0.337)
CC(work)	0.964 (0.477)	0.917 (0.588)	0.910 (0.719)
CC(free)	0.971 (0.494)	0.933 (0.588)	0.891 (0.597)
No. of atoms	3305	2781	6654
macromolecules	2799	2481	5707
ligands	83	77	296
solvent	423	233	651
Protein residues	377	335	758
RMS(bonds)	0.01	0.008	0.008
RMS(angles)	1.41	1.04	0.94
Ramachandran favored (%)	98.36	98.46	97.33
Ramachandran allowed (%)	1.37	1.54	2.54
Ramachandran outliers (%)	0.27	0	0.13
Rotamer outliers (%)	0	0.80	0.84
Clashscore	3.3	1.60	5.54
Average B-factor (Å^2)	32.2	45.96	21.46
macromolecules	31.14	46.05	20.52
ligands	32.9	49.86	32.26
solvent	39.11	43.55	24.82
Number of TLS groups		7	16

Highest-resolution shell statistics are in parentheses.

Supplementary Table 2: Crystallographic Statistics for VSG13

	VSG13	VSG13 + 0.5mM NaBr
Data Collection		
Beamline	ESRF ID29	Diamond i03
Processing software	iMosflm /CCP4 DIALS	iMosflm/CCP4 DIALS
Wavelength (Å)	1.0	0.9198
Resolution range (Å)	48.14-1.38 (1.43-1.38)	52.55-1.56 (1.62-1.56)
Space group	C 1 2 1	C 1 2 1
Unit Cell *a*, b, *c* (Å)	73.717 68.341 156.903 90	74.1477 68.4071 157.759 90
Unit Cell α, β, γ (°)	92.548 90	92.1646 90
Total reflections	465941 (45521)	432679 (21591)
Unique reflections	155980 (15141)	109295 (8780)
Multiplicity	3.0 (3.0)	4.0 (2.4)
Completeness (%)	97.09 (94.49)	97.22 (78.32)
Mean *I/sigma(I)*	8.07 (1.15)	18.77 (0.09)
Wilson B-factor	18.50	19.34
R-merge	0.04926 (0.6997)	0.1892 (4.641)
R-meas	0.05999 (0.8474)	0.2143 (5.751)
R-pim	0.03368 (0.4707)	0.09891 (3.314)
CC1/2	0.995 (0.84)	0.983 (0.06)
CC*	0.999 (0.955)	0.996 (0.336)
Refinement		
Refinement reflections	155980 (15092)	109211 (8755)
R-free reflections	1636 (159)	2019 (164)
R-work	0.2176 (0.4012)	0.2260 (0.3773)
R-free	0.2409 (0.4511)	0.2330 (0.3551)
CC(work)	0.949 (0.864)	0.901 (0.233)
CC(free)	0.947 (0.844)	0.899 (0.200)
No. of atoms	5782	5799
macromolecules	5256	5142
ligands	105	128
solvent	421	529
Protein residues	701	695
RMS(bonds)	0.011	0.009
RMS(angles)	1.12	0.95
Ramachandran favored (%)	97.67	98.09
Ramachandran allowed (%)	2.33	1.91
Ramachandran outliers (%)	0.00	0.00
Rotamer outliers (%)	0.71	0.00
Clashscore	2.81	4.23
Average B-factor (Å^2)	31.18	32.89
macromolecules	30.99	31.85
ligands	33.83	40.09
solvent	32.83	41.22
Number of TLS groups	0	28

Highest-resolution shell statistics are in parentheses.

Supplementary Table 3: Crystallographic Statistics for Mutant VSGsur

	VSGsur H122A	VSGsur H122A + 0.77mM suramin	VSGsur H122A + 7.7mM suramin
Data Collection			
Beamline	Diamond i03	SLS X06DA	SLS X06DA
Processing software	XIA2/DIALS (CCP4)	XIA2/DIALS (CCP4)	go.pi (XDS, POINTLESS)
Wavelength (Å)	0.9763	1.0	1.0
Resolution range (Å)	48.05 -1.47 (1.523-1.47)	38.08-1.75 (1.81-1.75)	39.16-1.66 (1.72-1.66)
Space group	P 21 21 2	P 21 21 2	P 21 21 2
Unit Cell *a*, b, *c* (Å)	47.0158 70.9113 130.677	46.90 70.95 130.44	46.94 71.03 130.61
Unit Cell α, β, γ (°)	90 90 90	90 90 90	90 90 90
Total reflections	995504 (99575)	588342 (59570)	686746 (66206)
Unique reflections	75170 (7360)	44210 (4304)	52136 (5028)
Multiplicity	13.2 (13.5)	13.3 (13.8)	13.2 (13.2)
Completeness (%)	99.28 (94.57)	98.94 (97.44)	99.79 (98.15)
Mean *I/sigma(I)*	12.12 (0.44)	16.67 (1.15)	19.44 (1.49)
Wilson B-factor	23.6	26.28	24.19
R-merge	0.09745 (2.95)	0.1224 (2.281)	0.0916 (1.719)
R-meas	0.1014 (3.067)	0.1273 (2.366)	0.0953 (1.788)
R-pim	0.02776 (0.8326)	0.03457 (0.6261)	0.0261 (0.4861)
CC1/2	1 (0.414)	0.999 (0.503)	1 (0.559)
CC*	1 (0.766)	1 (0.818)	1 (0.847)
Refinement			
Refinement reflections	74634 (6960)	44206 (4304)	52131 (5028)
R-free reflections	3654 (349)	2211 (215)	2605 (251)
R-work	0.2008 (0.3851)	0.178 (0.325)	0.185 (0.302)
R-free	0.2236 (0.3853)	0.207 (0.325)	0.208 (0.320)
CC(work)	0.959 (0.713)	0.9579 (0.725)	0.950 (0.787)
CC(free)	0.946 (0.633)	0.959 (0.726)	0.950 (0.738)
No. of atoms	3150	3067	2988
macromolecules	2749	2680	2644
ligands	83	72	61
solvent	318	315	283
Protein residues	368	359	356
RMS(bonds)	0.006	0.015	0.013
RMS(angles)	1.21	1.23	1.19
Ramachandran favored (%)	98.9	99.43	98.86
Ramachandran allowed (%)	1.1	0.57	1.14
Ramachandran outliers (%)	0	0	0
Rotamer outliers (%)	2.46	0.36	0
Clashscore	4.43	0.73	0.93
Average B-factor (Å^2)	38.44	39.22	38.91
macromolecules	38.26	38.90	38.86
ligands	39.85	36.81	30
solvent	39.6	42.47	41.31
Number of TLS groups	9	5	

Highest-resolution shell statistics are in parentheses.

SUPPLEMENTARY METHODS

1. Construction of pHH-VSG^{Sur}-hyg plasmid:

A switched variant of VSG termed VSG^{Sur} that emerged from *Trypanosoma brucei rhodesiense* culture under suramin selection has been reported to correlate with suramin resistance[2]. A DNA sequence encoding the VSG^{Sur} (GenBank: MF093647.1) was codon-optimized and synthesized as a pUC19 clone (BioCat, Germany). VSG^{Sur} DNA was PCR amplified from pUC19-VSG^{Sur} plasmid using Q5 DNA polymerase (New England Biolabs) and the following primers:

VSG^{Sur}-pHH-F1: CGACACGTACGCGGCATGCAAGCCGTAACACGC
VSG^{Sur}-pHH-R1: GAAATTTGAGGGGGGAAATTAAAAAAGCAAAAATGCAAGCAAAAGAGG

Also, a puromycin-resistant knock-in vector pHH-VSG3-PAC (PCT/EP2019/079063) was linearized by PCR using the following primers:

pHH-VSG2.3'-UTR-F1: TTTCCCCCCTCAAATTTCCCCCCTCC
pHH-VSG2-CTR-R1: ATGCCGCGTACGTGTCG

The VSG^{Sur} and pHH knock-in vector amplicons were assembled using HiFi® DNA Assembly Master Mix (New England Biolabs) according to the manufacturer's instructions, to replace VSG3 with VSG^{Sur}. To replace puromycin resistance with hygromycin, a hygromycine gene was PCR amplified from pHD789 plasmid[3] using the following primers:

Hyg-pHH-F1: GCTCTAGAACTAGTCAGCTTACCATGAAAAAGCCTGAACTCACCGCGAC
Hyg-pHH-R1: TGGGCAGGATCGATCCCTACTCTATTCCTTTGCCCTCGGACGAGTG

Also, the pHH knock-in vector excluding puromycin gene was linearized using the following primers:

Aldolase-3'-UTR-F2: GGATCGATCCTGCCCATTTGGCTTTTCCCTTGTCTCGTG
Actin-5'-UTR-R2: AGCTGACTAGTTCTAGAGCTTATTTTATGGCAGCAACGAGACCTTAC

Finally, the hyg gene and pHH knock-in vector amplicons were assembled using HiFi® DNA Assembly Master Mix (New England Biolabs) according to the manufacturer's instructions.

2. Generation of a *T. brucei* Lister427 Clone Expressing VSG^{Sur}:

A *T. brucei brucei* cell line expressing VSG2, termed 2T1[4], was transfected with EcoRV-linearized pHH-VSG^{Sur}-hyg plasmid to replace VSG2. Briefly, $2x10^7$ cells were electroporated with 10 µg DNA in 100 µl of a home-made Tb-BSF buffer[5] using Amaxa Nucleofector (Lonza), program X-001. After incubation in non-selective HMI-9 medium for 6 hours, hygromycin was added at 5 µg/ml and the cells were grown for 6 days at 37°C, 5% CO_2. Single clones isolated by serial dilution were screened for a VSG2-negative phenotype by FACS analysis using an APC-conjugated anti-VSG2 mouse mAb.

3. Generation of pHH-VSG vector for VSG Knock-in *T. brucei*:

Genomic DNA was extracted from VSG2-expressing 2T1 cells using DNAzol® reagent (Life Technologies) according to the manufacture's instruction. The VSG2 gene plus its upstream co-transposed region (CTR) and downstream telomere region were PCR amplified using Q5 DNA polymerase (New England Biolabs) and the following primers:

VSG2-CTR-F2: GAAGGCAGCGGAAAGTGTGCCAATGC
Tb427-tel-R2: AACACCTTAATCCGAAACACC

Also, pUC19 vector (Life Technologies) was linearized by PCR using the following primers:

pUC19-tel-F1: GATATCTCTAGAGTCGACCTGCAGGCATGCAAGC
pUC19-CTR-R2: ACTTTCCGCTGCCTTCGATATCGGATCCCCGGGTACCG

Additionally, telomere seeds were amplified by PCR from pSY-37F1D-CTR-BSD plasmid[6] using the following primers:

pSY.tel-F1: ACGGTGTTTCGGATTAAGGCCGCGGGAATTCGATTAGG
pSY.tel-R1: AGGTCGACTCTAGAGATATCGGATCCACTAGCTAGTGATTAAC

Finally, the above mentioned amplicons were assembled to make pHH-VSG2-Tel plasmid using HiFi® DNA Assembly Master Mix (New England Biolabs) following the manufacturer's instructions. In order to insert a puromycin resistance cassette, pHH-VSG2-Tel was linearized by PCR using the following primers:

pHH-VSG2-Tel-F1:
ATGGGGGGATATTAGACTTAGGCTTAGGATTAGGATTAGGATTAGGATTAGGGTTAATTTTTTCCTCTTT
TTTTTTAACTCACACCTCTATCCTG

pHH-VSG2-Tel-R1: GCTTGCATGCCGCGTTCGTG

Also, a puromycin resistance cassette was PCR amplified using the following primers:

pHH-PAC-F1: GGATTAGGCACAGCAAGGTCTTCTGAAATTCATGT
pHH-PAC-R1: CTAAGTCTAATATCCCCCCATTTTCTTCTTTTACATCA

The PCR amplicons from pHH-VSG2-Tel vector, and the puromycin cassette were assembled to make pHH-VSG2-PAC plasmid using HiFi® DNA Assembly Master Mix (New England Biolabs) following the manufacturer's instructions. To replace puromycin resistance with hygromycin, a hygromycine gene was PCR amplified from pHD789 plasmid[3] using the following primers:

Hyg-pHH-F1: GCTCTAGAACTAGTCAGCTTACCATGAAAAAGCCTGAACTCACCGCGAC
Hyg-pHH-R1: TGGGCAGGATCGATCCCTACTCTATTCCTTTGCCCTCGGACGAGTG

Also, the pHH knock-in vector excluding puromycin gene was linearized using the following primers:

Aldolase-3′-UTR-F2: GGATCGATCCTGCCCATTTGGCTTTTCCCTTGTCTCGTG
Actin-5′-UTR-R2: AGCTGACTAGTTCTAGAGCTTATTTTATGGCAGCAACGAGACCTTAC

Finally, the hyg gene and pHH knock-in vector amplicons were assembled using HiFi® DNA Assembly Master Mix (New England Biolabs) according to the manufacturer's instructions.

Alamar Blue assays

Serial drug dilutions were prepared on a 96-well plate and the parasites were added to a final concentration of 2×10^4cells/ml. After incubation for 68 hours, resazurin was added to a concentration of 11.4 μg/ml. The fluorescence of viable cells was determined after 3-4 hours with a SpectraMax reader (Molecular Devices) and SoftMax Pro 5.4.5 Software. Fitting of the dose-response curves (non-linear regression model, variable slope; four parameters, lowest value set to zero) and calculation of the IC50 values were carried out with GraphPad Prism 6.00.

Additional Information on VSGsur-Suramin Crystal Structure

The incubation of native crystals with suramin produced an unexpected effect on the crystal packing. Native VSGsur crystallized in the space group $P2_12_12$ with a single molecule in the asymmetric unit and a two-fold axis of crystallographic symmetry aligned with the dimerization axis, thereby producing a crystallographic dimer highly similar to that observed in other VSGs. One hour soaks of native crystals in 0.7 mM and 7.7 mM suramin did not change these parameters and led to structures where additional difference density appeared in the cavity but which could not be modeled. However, as the soak time increased (greater than 4 hours), a shift in the crystallographic symmetry was observed and correlated with increased evidence of electron density for suramin. In particular, the two-fold rotational symmetry no longer aligned with the dimerization axis of rotation, causing a shift in the contents of the crystal to harbor two molecules (a single homodimer of VSGsur) in the asymmetric unit in a lower symmetry space group. These changes were tolerated by the crystals, maintaining high diffraction, but led also to partial twinning (modeled in refinement with PHENIX with a twin operator (h, -k, -l) and a twin fraction of 19%). In these soaks, electron density for suramin was clear and able to be modeled.

A secondary suramin incubation state for VSGsur was also discovered in a minority of the crystals. In this state, H122 adopts the other possible conformer seen in the native structure. This conformation we term "closed" for how it reduces the size of the cavity (Supplementary Fig. 7b). In this closed conformation soak with suramin, the drug cannot occupy the same position as in the open conformation due to steric clash. Consistent with this, suramin does not occupy the binding site. We do observe difference density of a size possibly consistent with a molecule of the size of suramin, but it is positioned differently in a more extended conformation. However, the density is too weak to model with confidence and cannot even definitively be assigned to suramin. We hypothesize that as in the native structure, H122 is able to adopt two conformations, but that the open conformation with the stacking of the histidine rings over the

suramin benzene groups leads to the better ordered interaction and thus likely represents the only biological binding mode. The fact that ITC experiments show evidence for only one binding site is consistent with this. The closed conformation still leaves room for suramin perhaps to occupy the cavity, however, and the weak additional density observed in such structures may represent a transient state from solution to the stable binding mode.

Additional Discussion on VSGsur and Suramin Import

While VSGsur itself may act as an extracellular receptor for suramin, it is unlikely that it releases suramin into the cell in significant quantities given the high binding affinity and the fact that endocytosed VSGs are efficiently recycled back to the surface of the cell within a minute (see also discussion in Supplementary Methods). Consistent with this is the knowledge that VSGsur represents over 99% of the surface protein and dwarfs the concentration of other potential suramin importers; if VSGsur were to generally produce any net uptake into the cell, it should enhance the toxicity of suramin and not be associated with resistance. We therefore propose that any increased suramin uptake driven by extracellular VSGsur would be counterbalanced by the VSG recycling process, whereby those suramin molecules would be taken back to the surface as well. The amount of suramin taken in through other pathways would thus remain the majority of the compound that the intracellular targets are exposed to, even in VSGsur expressing cells. Even if at high suramin concentrations (e.g., near the IC_{50}) the existing VSGsur molecules are occupied by the extracellular suramin, the source of resistance can be the newly synthesized, unbound VSGsur dimers that the cell is constantly producing. The newly generated dimers could intercept free suramin in an endocytic compartment such as the sorting endosomes, as the trypanosome's endocytic and exocytic systems have a multitude of intersections.

Estimation of VSGsur-Suramin Export

Cells expressing VSG2 treated with a 200 nM dose of suramin accumulate an intracellular concentration of 1.8 μM suramin within 15 minutes[7]. This intracellular concentration eventually plateaus at a concentration approximately 2-3 fold higher than that[7]. VSGsur itself may act as an extracellular receptor for suramin. Therefore, the amount of suramin taken in through other importers likely remains the majority of the compound that the cell needs to resist in order to proliferate, even in VSGsur expressing cells (i.e., VSGsur is not an importer; see discussion above). As the existing VSGsur molecules are likely to be occupied by extracellular suramin, the source of resistance is thus likely the newly synthesized "clean" VSGsur dimers that the cell is constantly producing. The newly generated dimers could intercept free suramin in some endocytic compartment such as the sorting endosomes, as the trypanosome endocytic and exocytic systems have a multitude of intersections. The production rate of newly synthesized VSG has been estimated as equivalent to between 20,000[8] and 80,000[9] VSG monomers per minute. Therefore, with an estimated cell volume of ~30 cubic microns[10], we model the balance between suramin and available VSGsur molecules per cell below:

$$\text{Cell volume } 30\ \mu m^3 = 3x10^{-14}\ L$$

Number of suramin molecules imported in 15 minutes (normalizing the calculations to 15 minutes to match published literature on suramin import):

$(1.810^{-6}$ mol/L suramin) * $3x10^{-14}$ L = $5.4x10^{-20}$ mol

$5.4x10^{-20}$ mol * $6.022x10^{23}$ = $32.51x10^{3}$ = **32,510 suramin molecules**

Number of (unbound) VSGsur dimers produced per 15 minutes:

[(~20,000-80,000 monomers/min)]/2 * 15 min = **150,000-600,000 dimers**

Therefore, there is approximately a 5-20 fold excess of newly synthesized VSGsur available to export internalized suramin at an extracellular suramin concentration of 200 nM.

References

1. Bartossek, T. *et al.* Structural basis for the shielding function of the dynamic trypanosome variant surface glycoprotein coat. *Nat Microbiol* **2**, 1523–1532 (2017).
2. Wiedemar, N. *et al.* Beyond immune escape: a variant surface glycoprotein causes suramin resistance in *Trypanosoma brucei*: Suramin resistance in *T . brucei*. *Mol. Microbiol.* **107**, 57–67 (2018).
3. Irmer, H. & Clayton, C. Degradation of the unstable EP1 mRNA in Trypanosoma brucei involves initial destruction of the 3′-untranslated region. *Nucleic Acids Res.* **29**, 4707–4715 (2001).
4. Alsford, S. & Horn, D. Single-locus targeting constructs for reliable regulated RNAi and transgene expression in Trypanosoma brucei. *Mol. Biochem. Parasitol.* **161**, (2008).
5. Schumann Burkard, G., Jutzi, P. & Roditi, I. Genome-wide RNAi screens in bloodstream form trypanosomes identify drug transporters. *Mol. Biochem. Parasitol.* **175**, 91–94 (2011).
6. Pinger, J., Chowdhury, S. & Papavasiliou, F. N. Variant surface glycoprotein density defines an immune evasion threshold for African trypanosomes undergoing antigenic variation. *Nat Commun* **8**, 828 (2017).
7. Zoltner, M. *et al.* Suramin exposure alters cellular metabolism and mitochondrial energy production in African trypanosomes. *J. Biol. Chem.* **295**, 8331–8347 (2020).
8. Warren, G. Transport through the Golgi in Trypanosoma brucei. *Histochem. Cell Biol.* **140**, 235–238 (2013).
9. Manna, P. T., Boehm, C., Leung, K. F., Natesan, S. K. & Field, M. C. Life and times: synthesis, trafficking, and evolution of VSG. *Trends Parasitol.* **30**, 251–258 (2014).
10. Rotureau, B., Subota, I. & Bastin, P. Molecular bases of cytoskeleton plasticity during the Trypanosoma brucei parasite cycle. *Cell. Microbiol.* **13**, 705–716 (2011).